Journal of Magnetics 13(3), 81-84 (2008)

Spin Signals in Lateral Spin Valves with Double Nonmagnetic Bottom Electrodes

B. C. Lee*

Department of Physics, Inha University, Incheon 402-751, Korea

(Received 18 August 2008, Received in final form 3 September 2008, Accepted 4 September 2008)

Spin injection and detection in lateral spin valves with double nonmagnetic bottom electrodes are investigated theoretically. Spin-polarized current injected from a magnetic electrode is split to two bottom electrodes, and nonlocal spin signals between the other magnetic electrode and the nonmagnetic electrodes are calculated from drift-diffusion equations. It is shown that the spin signal is approximately proportional to the associated current in the electrode.

Keywords : spin injection, spin detection, lateral spin valve, nonlocal spin signal

1. Introduction

Spintronics has been a focus of interest for more than a decade [1]. Spin injection and detection are key elements for the development of spintronic devices [2, 3]. Nonlocal spin signal measurement provides a reliable method of spin detection because it excludes spurious effects such as anisotropic magnetoresistance [4-7]. A schematic sample structure for nonlocal spin signal measurement is shown in Figure 1(a). Two parallel ferromagnetic electrodes (FM1 and FM2) are grown on a nonmagnetic (NM) electrode in a lateral spin valve. Spin-polarized current is injected from the FM1 electrode and flows to the left side of the NM electrode. Voltage is measured between the FM2 electrode and the right side of the NM electrode and is denoted V_u, as shown in Figure 1(a). This voltage changes depending on the relative orientation of the FM1 and FM2 magnetizations, and the difference between parallel and anti-parallel configurations is proportional to the spin polarization of the injected current. For theoretical calculations, this nonlocal geometry is usually modeled by a one-dimensional circuit as shown in Figure 1(b) and solved with drift-diffusion equations [8-14]. This one-dimensional model describes the main features of the nonlocal spin signal fairly well, to some extent. Within the one-dimensional circuit approximation, the spin signals V_u and V_d shown in Figure 1(a) should be the same. The one-dimensional circuit approximation is valid when the width of the electrodes can be ignored. Recently, Ku *et al.* experimentally investigated the effect of finite NM electrode width w on the nonlocal spin signal [15]. They fabricated a series of Py/Au/Py lateral spin valves with different NM electrode widths, and observed the depen-

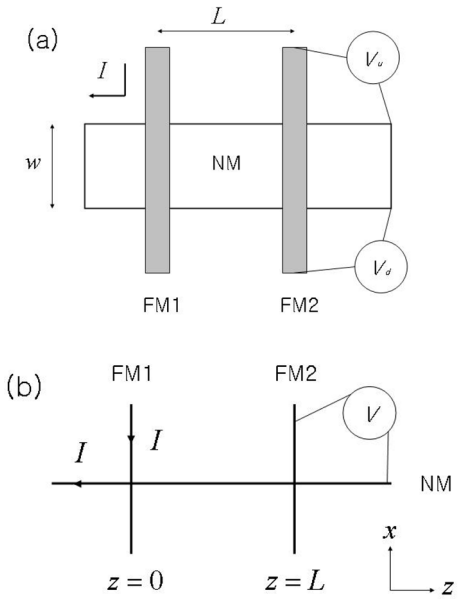

Fig. 1. (a) Nonlocal measurements in a lateral spin valve. A nonmagnetic electrode (NM) is at the bottom and two ferromagnetic electrodes (FM1 and FM2) are on the top. I is the electrical current, and V_u and V_d are nonlocal voltage measurements. w is the width of the bottom electrode and L is the distance between the two ferromagnetic electrodes. (b) One-dimensional approximation of the lateral spin valve shown in (a).

*Corresponding author: Tel: +82-32-860-7665
Fax: +82-32-872-7562, e-mail: chan@inha.ac.kr

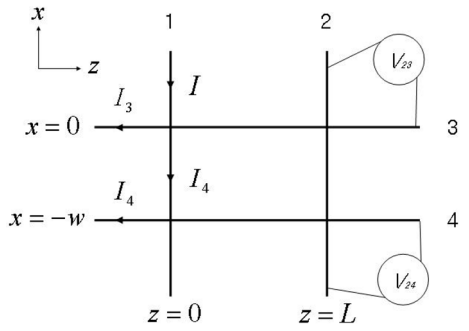

Fig. 2. One-dimensional schematic of a lateral spin valve with double nonmagnetic electrodes. Electrodes 1 and 2 (3 and 4) are ferromagnetic (nonmagnetic). I_3 (I_4) is the electric current in the left side of the nonmagnetic electrode 3 (4), and I is the total current ($I=I_3+I_4$). The distance between the two nonmagnetic electrodes is taken as w.

dence of the spin signals on w. It was found that the spin signals V_u and V_d are different, and that they show different behaviors as functions of width w. As w increases, V_u decreases rapidly at early stages and saturates to a small value later. On the other hand, V_d is weaker than V_u and eventually becomes zero.

In this paper, a lateral spin valve with two nonmagnetic bottom electrodes is investigated theoretically within a one-dimensional circuit model, as shown in Figure 2. Top electrodes 1 and 2 are ferromagnetic, and bottom electrodes 3 and 4 are nonmagnetic. We assume that the total current I, which flows from the top of magnetic electrode 1, splits at junction $x = 0$ and $z = 0$, and current I_3 (I_4) flows to the nonmagnetic electrode 3 (4) ($I = I_3 + I_4$). The nonlocal spin signal can be measured between ferromagnetic electrode 2 and nonmagnetic electrode 3 or 4. The current distribution in a finite NM electrode of real samples would not be uniform. For an accurate description, two- or three-dimensional sample structure needs to be taken into account. The two one-dimensional nonmagnetic current channels in our simple model (electrodes 3 and 4) might depict the nonuniform current distribution in a finite NM electrode. The distance between electrodes 3 and 4 is taken as w.

This paper is organized as follows. In Section 2, the drift-diffusion equations are applied to the lateral spin valves with two nonmagnetic bottom electrodes, and a detailed calculation is described. In Section 3, results are presented with discussion.

2. Theoretical Model

Drift-diffusion equations are adopted to describe spin-dependent transport in the lateral spin valve with two nonmagnetic bottom electrodes shown in Fig. 2. The spin-dependent current density $\vec{J}_\sigma$ and electrochemical potential μ_σ are obtained from

$$\vec{J}_\sigma = \frac{1}{e\rho_\sigma}\vec{\nabla}\mu_\sigma, \tag{1}$$

$$\vec{\nabla}\cdot(\vec{J}_+ + \vec{J}_-)=0, \tag{2}$$

$$\nabla^2(\mu_+ - \mu_-)=\frac{\mu_+ - \mu_-}{\lambda^2}. \tag{3}$$

Here, σ is the spin index ($\sigma = +$ is for up-spin and $\sigma = -$ is for down-spin), ρ_σ is the spin-dependent resistivity, and λ is the spin diffusion length. For simplicity, it is assumed that the same ferromagnetic (nonmagnetic) materials are used for electrodes 1 and 2 (3 and 4), and the junction areas are the same. The resistivity and spin-diffusion length in the magnetic (nonmagnetic) material are denoted as ρ_F (ρ_N) and λ_F (λ_N), respectively. β_F is the spin polarization of the electrical current in bulk magnetic material, and γ is the spin polarization for the tunneling of electrons at the ferromagnetic and nonmagnetic interface. A_J is the junction area, and A_N is the cross-sectional area of the nonmagnetic electrode.

The electrochemincal potential $\mu_{i\sigma}$ in electrode i (i = 1, 2, 3, 4) can be expressed as

$$\mu_{1\pm}(x)=\begin{cases} -e\rho_F\dfrac{I}{A_J}x - er_F(\pm1-\beta_1)\dfrac{B_1}{2}e^{-x/\lambda_F} - eV_1, & x>0, \\ -e\rho_F\dfrac{I_4}{A_J}x + er_F(\pm1-\beta_1)\left(\dfrac{C_1}{2}e^{x/\lambda_F} - \dfrac{D_1}{2}e^{x/\lambda_F}\right) - eV_1, & -w<x<0, \\ er_F(\pm1-\beta_1)\dfrac{E_1}{2}e^{(x+w)/\lambda_F} - eV_1, & x<-w, \end{cases}$$

$$\mu_{2\pm}(x)=\begin{cases} -er_F(\pm1-\beta_2)\dfrac{B_2}{2}e^{-x/\lambda_F} - eV_2, & x>0, \\ -er_F(\pm1-\beta_2)\left(\dfrac{C_2}{2}e^{x/\lambda_F} - \dfrac{D_2}{2}e^{-x/\lambda_F}\right) - eV_2, & -w<x<0, \\ er_F(\pm1-\beta_2)\dfrac{E_2}{2}e^{(x+w)/\lambda_F} - eV_2, & x<-w, \end{cases}$$

$$\mu_{3\pm}(z)=\begin{cases} -e\rho_N\dfrac{I_3}{A_N}z \pm er_N\dfrac{B_3}{2}e^{z/\lambda_N} - eV_3, & z<0, \\ \pm er_N\left(\dfrac{C_3}{2}e^{z/\lambda_N} - \dfrac{D_3}{2}e^{-z/\lambda_N}\right) - eV_3, & 0<z<L, \\ \mp er_N\dfrac{E_3}{2}e^{-(z-L)/\lambda_N} - eV_3, & z>L, \end{cases}$$

$$\mu_{4\pm}(z)=\begin{cases} -e\rho_N\dfrac{I_4}{A_N}z \pm er_N\dfrac{B_4}{2}e^{z/\lambda_N} - eV_4, & z<0, \\ \pm er_N\left(\dfrac{C_4}{2}e^{z/\lambda_N} - \dfrac{D_4}{2}e^{-z/\lambda_N}\right) - eV_4, & 0<z<L, \\ \mp er_N\dfrac{E_4}{2}e^{-(z-L)/\lambda_N} - eV_4, & z>L, \end{cases}$$

where β_i is the bulk spin-polarization of electrode i (i=1, 2 and $\beta_i = \pm\beta_F$ depending on the magnetization direction), $r_F = \rho_F\lambda_F/(1-\beta_F^2)$, and $r_N = \rho_N\lambda_N$. Coefficients B_i, C_i, D_i, E_i, and V_i (i=1, 2, 3, 4) are determined from the boundary conditions. The spin-dependent current density is easily obtained from the electrochemical potential using Eq. (1). For example, the spin-dependent current density $J_{1\pm}$ in electrode 1 is

$$J_{1\pm}(x)=\begin{cases} -\dfrac{1\pm\beta_1}{2}\dfrac{I}{A_J}\pm\dfrac{B_1}{2}e^{-x/\lambda_F}, & x>0, \\ -\dfrac{1\pm\beta_1}{2}\dfrac{I_4}{A_J}\pm\left(\dfrac{C_1}{2}e^{x/\lambda_F}+\dfrac{D_1}{2}e^{-x/\lambda_F}\right), & -w<x<0, \\ \pm\dfrac{E_1}{2}e^{(x+w)/\lambda_F}, & x<-w. \end{cases}$$

For the calculation, it is easier to use spin current $J_{i,s}(x) \equiv J_{i+}(x) - J_{i-}(x)$ (i = 1, 2, 3, 4) and the difference of the electrochemical potentials between up and down spins $\Delta\mu_i(x)\equiv\mu_{i+}(x)-\mu_{i-}(x)$ (i = 1, 2, 3, 4). Then, for electrode 1, we have

$$J_{1s}(x)=\begin{cases} -\beta_1\dfrac{I}{A_J}+B_1e^{-x/\lambda_F}, & x>0, \\ -\beta_1\dfrac{I_4}{A_J}+C_1e^{x/\lambda_F}+D_1e^{-x/\lambda_F}, & -w<x<0, \\ E_1e^{(x+w)/\lambda_F}, & x<-w, \end{cases}$$

$$\Delta\mu_1(x)=\begin{cases} -2er_FB_1e^{-x/\lambda_F}, & x>0, \\ 2er_F(C_1e^{x/\lambda_F}-D_1e^{-x/\lambda_F}), & -w<x<0, \\ 2er_FE_1e^{(x+w)/\lambda_F}, & x<-w. \end{cases}$$

Similarly, for electrode 3, we have

$$J_{3s}(z)=\begin{cases} B_3e^{z/\lambda_N}, & z>0, \\ C_3e^{z/\lambda_N}+D_3e^{-z/\lambda_N}, & 0<z<L, \\ E_3e^{-(z-L)/\lambda_N}, & z>L, \end{cases}$$

$$\Delta\mu_3(z)=\begin{cases} 2er_NB_3e^{z/\lambda_N}, & z>0, \\ 2er_N(C_3e^{z/\lambda_N}-D_3e^{-z/\lambda_N}), & 0<z<L, \\ -2er_NE_3e^{-(z-L)/\lambda_N}, & z>L. \end{cases}$$

Since $\mu_{1\pm}(x)$ is continuous along the x-axis, so is $\Delta\mu_1(x)$, and then the relations $-B_1=C_1-D_1$ and $C_1e^{-w/\lambda_F}-D_1e^{w/\lambda_F} = E_1$ are obtained. Similar relations are obtained for other coefficients from continuity of $\Delta\mu_i(i$=2, 3, 4). The other relations are obtained from current conservation. Let us consider the junction at x=0 and z=0 which involves electrodes 1 and 3. Tunneling current $J_{t\pm}(x$=0, z=0) is related to the electrochemical potentials as follows:

$$\mu_{3\pm}(z=0)-\mu_{1\pm}(x=0)=2e(1\mp\gamma_1)\,r_I\,J_{t\pm}(x=0,\ z=0),$$

where γ_1 is the spin polarization for tunneling current at the junction x=0 and z=0 ($\gamma_1 = \pm\gamma$ depending on the magnetization directions of electrode 1), and $r_I = r_I^0/(1-\gamma^2)$ where r_I^0 is the tunneling resistance per unit area at the junction. The sign of $J_{t\pm}(x$=0, z=0) is positive when the current flows from electrode 1 to electrode 3. From current conservation at the junction, we have

$$\begin{aligned} J_{t,s}(x=0,\ z=0)&=J_{1s}(x=0-)-J_{1s}(x=0+) \\ &=(A_N/A_J)[J_{3s}(z=0+)-J_{3s}(z=0-)], \end{aligned}$$

where $J_{t,s}=J_{t+}-J_{t-}$, and we obtain the relations

$$r_NB_3+r_FB_1=r_I[-(-\beta_1I/A_J+B_1)+(-\beta_1I_4/A_J+C_1+D_1)]-\gamma_1r_II_4/A_J,$$

$$A_J[-\beta_1I/A_J+B_1-(-\beta_1I_4/A_J+C_1+D_1)]=A_N[B_3-(C_3+D_1)].$$

In a similar way, the other relations between coefficients are obtained from the remaining junctions. It can be shown that voltage difference $V_{23(24)}$ between electrodes 2 and 3 (4) are expressed as

$$V_{23}=V_2-V_3=-\frac{1}{2e}\beta_2\Delta\mu_2(x=0)-\gamma_2[J_{2s}(x=0-)-J_{2s}(x=0+)],$$

$$V_{24}=V_2-V_4=-\frac{1}{2e}\beta_2\Delta\mu_2(x=-w)-\gamma_2[J_{2s}(x=-w-)-J_{2s}(x=-w+)],$$

where γ_2 is the spin polarization for tunneling at the junction between electrode 2 and nonmagnetic electrode 3 or 4. Finally, V_{23} and V_{24} are expressed with coefficients as

$$V_{23}=\beta_2r_FB_2-\gamma_2r_I(C_2+D_2-B_2),$$

$$V_{24}=-\beta_2r_FE_2+\gamma_2r_I(C_2e^{-d/\lambda_F}+D_2e^{d/\lambda_F}-E_2).$$

The nonlocal spin signals are obtained after the coefficients are calculated from the linear simultaneous equations.

3. Results and Discussion

First, we briefly analyze the one-dimensional circuit model with one bottom electrode shown in Fig. 1(b). The nonlocal spin signal ΔR_s for this system is given by $\Delta R_s=\Delta V/I$, where ΔV is the voltage difference between parallel and anti-parallel magnetizations. The calculation method is exactly same as that in Section 2, and the nonlocal spin signal is

$$\Delta R_s=R_Ne^{-L/\lambda_N}\frac{(\beta_FR_F/2+\gamma R_I)^2}{(R_F/2+R_I+R_N/2)^2-(R_N/2)^2e^{-2L/\lambda_N}},$$

where $R_N=r_N/A_N=\rho_N\lambda_N/A_N$, $R_F=r_F/A_J=\rho_F\lambda_F/(1-\beta_F^2)A_J$, and $R_I=r_I/A_J=r_I^0/(1-\gamma^2)A_J$. This result is different from that in [13] by the factor 1/2 associated with R_F. This is because the magnetic electrodes have both top and bottom sides in our case, as shown in Fig. 1(b), whereas the lower side has been ignored in [13]. The spin current flows both up and down the sides of the ferromagnetic

electrodes in our model, resulting in the factor 1/2, similar to the factor 1/2 associated with R_N. When e^{-2L/λ_N} is neglected, which is often a good approximation for real samples, the nonlocal signal has a simple form such as

$$\Delta R_s \approx R_N e^{-L/\lambda_N} \frac{(\beta_F R_F/2+\gamma R_I)^2}{(R_F/2+R_I+R_N/2)^2}.$$

The nonlocal signals in the lateral spin valve with double nonmagnetic electrodes as shown in Fig. 2 are denoted as $\Delta R_{23}=\Delta V_{24}/I$ and $\Delta R_{24}=\Delta V_{24}/I$. The exact expressions of ΔR_{23} and ΔR_{24} are complicated. Thus, we provide only approximate results by assuming e^{-L/λ_N} and e^{-w/λ_F} are very small. Then, the nonlocal spin signals are

$$\Delta R_{23} \approx R_N e^{-L/\lambda_N} \frac{(\beta_F R_F/2+\gamma R_I)^2}{(R_F/2+R_I+R_N/2)^2} \frac{I_3}{I},$$

$$\Delta R_{24} \approx R_N e^{-L/\lambda_N} \frac{(\beta_F R_F/2+\gamma R_I)^2}{(R_F/2+R_I+R_N/2)^2} \frac{I_4}{I}.$$

The results are exactly the same as those of the one-dimensional circuit model with one bottom electrode, except for the factors I_3/I and I_4/I. In other words, the spin signal is proportional to the associated electric current. With this result, the experimental investigation in [15] might be explained qualitatively. In the bottom electrode with finite width w shown in Fig. 1(a), the electrical current density on the left side would not be uniform. I_3 and I_4 in our model may be related to the current density at the upper and lower part of the finite bottom electrodes, respectively. The current density distribution will change as a function of w. The current density distribution may be calculated once the lateral spin valve is given, but we provide a qualitative description here because our model is already greatly simplified. We always expect that I_3 is larger than I_4 because the resistance is higher for the longer current path. When w is very small in the finite NM electrode, the current density is large overall for the fixed current I, and it is expected that the difference in current density between the upper and lower parts of the electrode is small because the current paths are almost the same. Then, I_3 and I_4 are large, and both the nonlocal spin signals ΔR_{23} and ΔR_{24} are strong. As w increases, the current density in the finite NM electrode in Fig. 1(a) will decrease rapidly overall due to the increase of the cross-sectional area for fixed current I. The decrease in current density will be more pronounced at the lower part because the current path for the lower part increases continuously, while the current path is fixed for the upper part. As w increases further, the current density at the upper side will saturate, while the current density at the lower part goes to zero as the current path continuously increases. Thus, the current density change as a function of w explains qualitatively the main feature of the experimental results in [15].

Acknowledgement

This work was supported by Inha University Research Grant.

References

[1] G. A. Prinz, Science **282**, 1660 (1998).
[2] (a) M. Johnson and R. H. Silsbee, Phys. Rev. Lett. **55**, 1790 (1985). (b) Phys. Rev. B **35**, 4959 (1987), (c) ibid. **37**, 5312 (1988).
[3] J.-H. Han, J.-W. Lee, and C.-Y. You, J. Magnetics **12**, 77 (2007).
[4] F. J. Jedema, A. Filip, and B. J. van Wees, Nature (London) **410**, 345 (2001).
[5] F. J. Jedema, M. S. Nijboer, A. T. Filip, and B. J. van Wees, Phys. Rev. B **67**, 085319 (2003).
[6] J. Hamrle, T. Kimura, Y. Otani, K. Tsukagoshi, and Y. Aoyagi, Phys. Rev. B **71**, 094402 (2005).
[7] J.-H. Ku, J. Chang, H. C. Koo, J. Eom, S. H. Han, and G.-T. Kim, J. Magnetics **12**, 152 (2007).
[8] P. van Son, H. van Kampen, and P. Wyder, Phys. Rev. Lett. **58**, 2271 (1987).
[9] T. Valet and A. Fert, Phys. Rev. B **48**, 7099 (1993).
[10] S. Hershfield and H. L. Zhao, Phys. Rev. B **56**, 3296 (1997).
[11] G. Schmidt, D. Ferrand, L. W. Molenkamp, A. T. Filip, and B. J. van Wees, Phys. Rev. B **62**, R4790 (2000).
[12] A. Fert and H. Jaffres, Phys. Rev. B **64**, 184420 (2001).
[13] S. Takahashi and S. Maekawa, Phys. Rev. B **67**, 052409 (2003).
[14] B. C. Lee, J. Korean Phys. Soc. **47**, 1093 (2005).
[15] J.-H. Ku, J. Chang, J. Eom, H. C. Koo, S. Han, and G. T. Kim, KMS 2008 summer conference.